

*The Institute of Astronomy & Geophysics  
of Mongolian Academy of Sciences*

# Book of Extended Abstracts

The International Conference on Astronomy  
and Geophysics in Mongolia, 2017

Ulaanbaatar, Mongolia  
20-22 July, 2017

1957-2017  
**60 YEARS**

**PROCEEDINGS OF THE INTERNATIONAL  
CONFERENCE ON ASTRONOMY & GEOPHYSICS  
IN MONGOLIA, 2017**

20-22 JULY, 2017, ULAANBAATAR, MONGOLIA

**Extended Abstract Volume**

**Editors in chief**

*(Institute of Astronomy and Geophysics, Ulaanbaatar, Mongolia)*

**Prof. Demberel Sodnomsambuu**

**Dr. Odonbaatar Chimed**

**Dr. Ulziibat Munkhuu**

Ulaanbaatar  
2017

DDC  
551.22  
P-23

**INSTITUTE OF ASTRONOMY AND GEOPHYSICS OF MONGOLIAN  
ACADEMY OF SCIENCES (IAG, MAS)**

Editors: Dr Odonbaatar Chimed  
Dr Munkhsaikhan Adiya  
Mrs Ankhtsetseg Dorjsuren

Print design: Mungunshagai Mendbayar

**ISBN 978-99978-1-236-0**

Published by Mongol Altay printing Co.ltd

## INVESTIGATION OF THE BOUNDARY AND INTERNAL FAULT ZONES OF TUNKA BASIN (BAIKAL RIFT SYSTEM) USING HVSR METHOD

Sankov A.V.<sup>1</sup>, Dobrynnina A.A.<sup>1,2</sup>, Chernykh E.N.<sup>1</sup>, Sankov V.A.<sup>1,3</sup> and  
Shagun A.N.<sup>1</sup>

<sup>1</sup> Institute of the Earth Crust of Siberian Branch of Russian Academy of Sciences, Irkutsk, Russia

<sup>2</sup> Geological Institute of Siberian Branch of Russian Academy of Sciences, Ulan-Ude, Russia

<sup>3</sup> Irkutsk State University, Irkutsk, Russia

*Contact:* alekseysankov@inbox.ru

### Introduction

This work is devoted to the study of the Tunka basin structure of south-western flank of the Baikal rift system. This basin is the central element of 160km long latitudinal chain of rift basins separated by low uplifts. Tunka is the largest and deepest basin (Fig. 1). The thickness of sedimentary cover is greater than 2000 meters (Logatchev, Zorin, 1978). The sedimentary cover of the basin is represented by rift lacustrine, alluvial, volcanoclastic sediments and basalt flows. In general the depression is a half-graben bounded from the north by the steeply dipping Tunka fault. The surface of the Khamar-Daban block from the south gently plunges under the sediments of the depression. It is assumed under sediments the depression is crossed by the seismically active Baikal-Mondy fault in a latitudinal direction. Several known historical and instrumentally recorded strong earthquakes are confined to this fault.

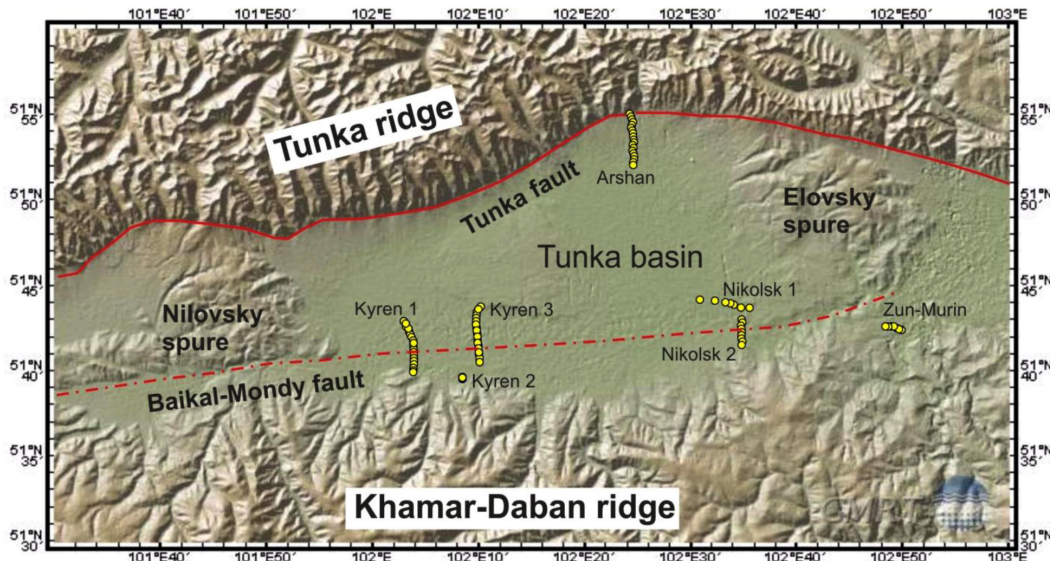


Figure 1: The topography of Tunka basin. The position of the HVSR profiles is shown by yellow circles.

### Method

We used the data of microseismic sounding in comparison with the data of drilling and structural observations. The Horizontal-to-Vertical Spectral Ratio (HVSR) method, also called Nakamura's method (Nakamura, 1989), is a single-station approach using ambient noise measurements to estimate the fundamental frequency of a site. For site conditions where there is a strong contrast in velocity between the surface layer and a deeper material a peak will be observed in the HVSR plot that closely corresponds to the fundamental frequency of the site. This method has been used extensively in microzonation studies of cities around the world. At present the number of publications

on the use of various modifications of microseismic sounding for the study of different parts of the earth's crust are known (Gorbatikov et al., 2008; Gosar, Lenart, 2010; Mulargia, Castellaro, 2016). The method allows to evaluate of the position of faults, forms the basement, to reveal heterogeneity of medium.

When studying the internal structure of rift basins and active fault zones, measurements of ambient noise were made for long profiles crossing the depressions, as well as for profiles oriented across the orientation of fault zones. The recording time of ambient noise in each point was from 30 minutes or more. The  $H/V$ -ratio curves were calculated in the frequency range from 0.5 to 20 Hz. The velocity structure was estimated using dispersion curves calculated for single or two stations located in the same block.

## Results

In the present study we consider several profiles (Fig. 1). Sounding profiles were traversed in the inner parts of basins, as well as across strike of boarder faults.

The submeridional profile of Nikolsk 2 in the southern side of the Tunka depression crossing the zone of the Baikal-Mondy fault is a good illustration of the HVSR method. (Fig. 1). The thickness of the sedimentary cover here increases in the north. At the same time the complexity of the section increases due to the appearance of dense inhomogeneities (Fig. 2, 3). It is reflected on  $H/V$  curves in the appearance of additional maxima of the  $H/V$  ratio values. The results obtained were compared with drilling data (Fig. 3). The zone of the Baikal-Mondy fault is represented by three faults in the basement that emerge into the sedimentary cover.

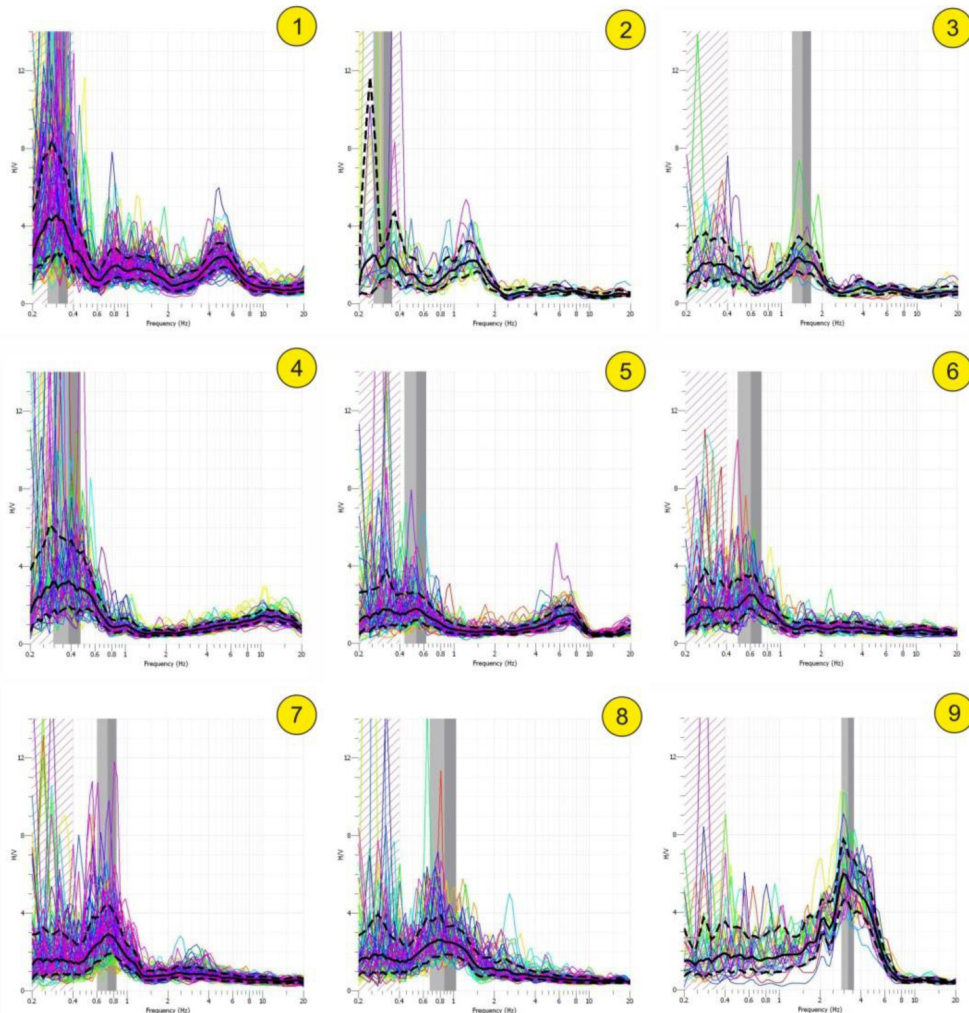


Figure 2:  $H/V$  curves for seismic stations of Nikolsk 2 profile.

Sublatitudinal cross-section along the left side of the Irkut river valley in the east of Tunka basin (Nikolsk 1, Fig. 1) shows large differences in the composition and the constitution of one in the eastern and western parts. West, the deepest part of the basin, is composed by mainly of soft, and at the bottom - denser sediments. Basement depth here is about 1000 meters. To the east an uplift of basement reveals along the fault of reverse or thrust type, or the existence of dense body of volcanic rocks in the lower part of the section. Still further to the east there is a gradual rise of the basement, which corresponds to the modern relief of the western slope Elovsky spur. Here, in the upper part of the section high density layers are allocated, which correspond to basalt flows established by drilling and geological observations.

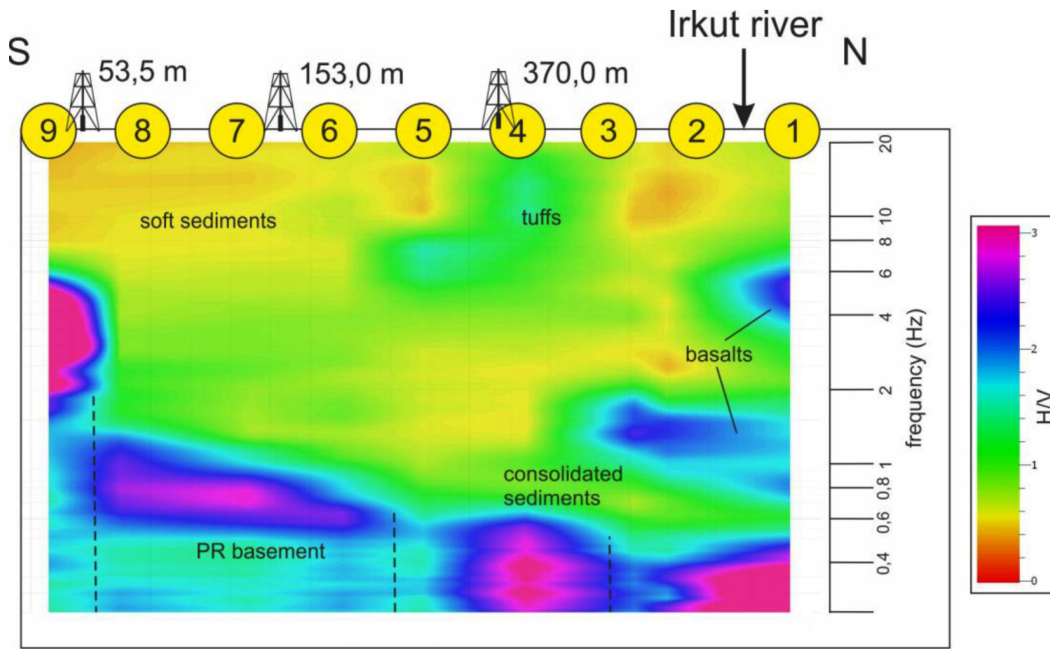


Figure 3: The HV cross-section along Nikolsk 2 profile. The position and depths of boreholes are shown. Dashed lines show the faults in the basement.

Two submeridional profiles in the western part of the basin (Fig. 1) made it possible to determine the position of individual faults in the zone of the Baikal-Mondy fault. According to our data, the general structure of this zone is a graben, the depth of which exceeds 1200m. The graben is complicated by a longitudinal fault, along which vertical displacement of the surface of the PR basement of the depression is also noted.

The preliminary interpretation of submeridional 6km long section across Tunka fault (Arshan) shows the vertical displacement of basement surface with amplitude at about first tens meters along the fault plane. Further to the south on 5km the inclined step is traced. Obviously, the main displacement which forms a deep part of the basin is located to the south of the end of the profile.

## Conclusions

As a result of the investigation, we came to the following conclusions:

1. The use of the method of microseismic profiling made it possible to establish the position of individual faults in the zone of the seismically active Baikal-Mondy fault under the KZ sediments of the Tunka rift basin. In addition, it allows to determine the thickness of the sediments.
2. There are the fundamental differences in the compositions of the section in the western and eastern parts of the Tunka basin. Western (the deepest part) of the basin obviously does not contain basalt flows.

The reported study was funded by RFBR according to the research project 17-05-00826.

## References

- [1] Logatchev N.A., Zorin Yu.A., 1987. Evidence and causes of the two-stage development of the Baikal rift // Tectonophysics, 143(1-3): 225-234.
- [2] Nakamura Y., 1989. A method for dynamic characteristics estimation of subsurface using microtremor on the ground surface. QR Railw. Tech. Res. Inst., 30: 25–33.
- [3] Gorbatikov A. V., Stepanova M. Yu., Korablev G. E., 2008 Microseismic field affected by local geological heterogeneities and microseismic sounding of the medium. Izv. Phys. Solid Earth 44 (7), 577–592.
- [4] Gosar A., Lenart A., 2010. Mapping the thickness of sediments in the Ljubljana Moor basin (Slovenia) using microtremors. Bulletin of Earthquake Engineering, 8. P. 501-518.
- [5] Mulargia F., Castellaro S. 2016. HVSR deep mapping tested down to 1.8 km in Po Plane Valley, Italy. Physics of the Earth and Planetary Interiors, 261. P.17–23.

## CONTENTS

<b>Astronomy, astrophysics and space science .....</b>	<b>09</b>
Owl telescope in Mongolia .....	11
Observation of the coronal green line at a wavelength of 5303Å .....	12
The results of wavelet analysis application to variations of the Earth rotation parameters .....	13
Observation of solar radio bursts .....	14
The minor planets in the solar system .....	15
Intensity of solar ultraviolet radiation in Ulaanbaatar regions and comparative analysis of some characteristics of climatic conditions in the places of Khurel-Togoot and Tavan tolgoi .....	16
A fuzzy neural network model in analyzing the air pollution factors .....	19
Dynamic phenomena in the active regions of 24-th solar cycle .....	26
The optical afterglow observations of gamma-ray bursts .....	31
Solar active phenomena observation .....	32
Meteor observation in Irkutsk region .....	33
Mongolian-Russian cooperation at the Khurel-Togoot observatory in the ison project framework ..	34
A study of image prediction for yield mapping in real environment .....	35
 <b>Geomagnetism .....</b>	 <b>41</b>
Monitoring of the geomagnetic field variations at the high - mountain biospheric station dzhuga and forecasting of natural disasters and extreme weather .....	43
Probing the Earth's mantle using satellite and ground - based magnetic data. Progress status and challenges .....	44
Towards geophysical exploration of geothermal resources in the Hangai Mountains .....	45
High-precision Overhauser magnetometers applications .....	46
Variations of earthquake focal mechanism types in northern tien shan .....	53
Tectonomagnetic monitoring of crustal stress state in the baikal rift zone and some results for study of the kultuk earthquake .....	54
Rigid blocks in the earth's crust and strong earthquakes .....	59
The monitoring of geomagnetic field in the Baikal-Hubsugul fault in 2010-2015 .....	63
Geophysical complex ISTP SB RAS for monitoring electromagnetic fields in high and middle latitudes ..	64
Study of the Magnetic Field Response due to Geodynamic Processes in Central Mongolia (Emeelt) and Russia (North-West Caucasus) .....	65
The heat flows via CPD .....	74
 <b>Geodynamics, active deformation, GPS, active fault, paleoseismology .....</b>	 <b>79</b>
Identification and characterization of the Sharkhai and Avdar active faults near Mongolia's capital city: Impact on Seismic Hazard Assessment in a low deformation setting .....	81
Co-seismic moment released by the surface rupturing 1934 bihar-nepal earthquake .....	87
Stress fields in the area of the Mogod earthquake in Mongolia from the structural paragenetic analysis of tectonic fracturing .....	88
Wave dynamics of rock deformations according results of monitoring .....	94
Numerical reconstruction of normal-fault scarps evolution .....	99
Radon monitoring of ulaanbaatar region .....	103
Cosmogenic $^{36}\text{Cl}$ geochronology of offset terraces along the Ovacık Fault (Malatya-Ovacık Fault Zone, Eastern Turkey): Implications for the intraplate deformation of the Anatolian Scholle .....	104
Tropospheric delay of GPS signals and their connection with the level of moisture content within the Baikal region and the Selenga river basin .....	105
Geodynamics of northern Mongolian and Transbaikalian segments of the Central Asian Orogenic Belt at	

<i>Late Paleozoic – Mesozoic</i> . . . . .	111
<i>GPS developments in mongolia and its applications in geodynamic studies</i> . . . . .	112
<i>Gheological hazard assessment of the Ulaanbaatar agglomeration</i> . . . . .	113
<i>Structural characteristics of the Hovd fault zone, Mongolian Altaid region, western Mongolia</i> . . . . .	114
<i>Cumulative deformation by multiple surface-faulting earthquakes on the Bulnay Fault, Mongolia: A preliminary investigation</i> . . . . .	120
<i>Mapping of active faults in Korea by airborne LiDAR survey: A preliminary investigation</i> . . . . .	121
<i>Slip rates and ages of past earthquakes along the main western Gobi-Altay active slip faults (Gobi-Altay, Mongolia)</i> . . . . .	122
<i>Quantifying the differential uplift on the western branches of the north Anatolian fault: Sakarya river terraces, NW turkey</i> . . . . .	124
<i>Horizotal slip distribution through several seismic cycles the eastern Bogd fault, Gobi-Altai, Mongolia</i> . . . . .	129
<i>Impact of cosmic factors on the Baikal rift zone seismic regime</i> . . . . .	131
<i>Studying active faults by GPR technique; example of Songino fault Ulaanbaatar</i> . . . . .	137
<i>Present-day movements of the earth's crust of Mongolia from GPS measurements at the permanent sites</i> . . . . .	143
<i>First results of GPS measurements within the local networks in the Central Mongolia</i> . . . . .	147
<i>Songino active fault from GPR imaging and trench results, Ulaanbaatar, Mongolia</i> . . . . .	152
<i>The crustal state of stresses and the conditions of the tectonic structures activation of Southeast Mongolia in the Cenozoic</i> . . . . .	158
<i>Recurrence of strong earthquakes in the active Hovd fault zone, Mongolian Altay</i> . . . . .	163
<i>Tectonic position and geological manifestations of the 1967 Mogod earthquake, Mongolia</i> . . . . .	165
<i>Estimation of the recent activity of large faults in the Ulaanbaatar and Mogod geodynamic testing areas in Central Mongolia based on soil-radon data</i> . . . . .	166
<i>Active faults and Late Cenozoic crustal stress state in the central part of Mongolia</i> . . . . .	171
<i>Wave dynamics of seismicity in the annual cycles in the southeastern segment of the Amurian plate</i> . . . . .	176
<i>High-resolution surface rupture map and slip distribution of the 1905 <math>M \geq 8</math> Tsetserleg-Bulnay strike-slip earthquake sequence, Mongolia</i> . . . . .	181
<i>Intraplate geodynamics in Mongolia: constraints from geochronology, thermochronology, and geochemistry</i> . . . . .	182
<b>Large intra-continental earthquakes: Source characteristics, seismic activity, historical earthquakes</b> . . . . .	<b>183</b>
<i>Preliminary result of earthquake hypocenter determination using new 1d velocity model: khuvsugul area</i> . . . . .	185
<i>Seismicprofiling in a zone of mogod fault</i> . . . . .	186
<i>Mongolian National Seismic Network and its operations</i> . . . . .	189
<i>Lg-wave cross correlation applied to detection and location of events in high-seismicity regions of mainland east asia</i> . . . . .	190
<i>Earthquake Monitoring: Automatic processing at the Mongolian National Seismic Network</i> . . . . .	196
<i>Tectonophysical analysis of seismic hazard of faults in Central asia</i> . . . . .	197
<i>Focal mechanisms of aftershocks of <math>Mw = 4.59</math>, Bayanbulag earthquake</i> . . . . .	198
<i>A mechanism causing temporal variation in b-values Prior to a mainshock</i> . . . . .	199
<i>Ambient noise monitoring in Ulaanbaatar region</i> . . . . .	203
<i>Paleoseismic investigation on the eastern end of the Altyn Tagh fault</i> . . . . .	207
<i>Seismic activity of the Emeelt fault area investigated using tomoDD</i> . . . . .	208
<i>The seismicity of the south Hangay dome of central Mongolia: 1-d velocity model for the area from local earthquake data</i> . . . . .	209

<i>Radionuclide analysis of the CTBTO's IMS stations data in Mongolia . . . . .</i>	210
<i>Reference one dimensional velocity model and precise locations of local earthquake hypocenters in the hangay region . . . . .</i>	211
<i>Precise location of seismicity in and around Bulnay fault . . . . .</i>	212
<i>Detection capability of infrasound station . . . . .</i>	213
<i>Ground Penetrating Radar result of data analysis For Songino active fault, Ulaanbaatar . . . . .</i>	214
<i>Discrimination of earthquakes and explosions around north korean nuclear test site . . . . .</i>	215
 <b><i>Crustal and lithosphere structures . . . . .</i></b>	<b>221</b>
<i>Deep structure of the baikal rift system Based on the seismic wave attenuation . . . . .</i>	223
<i>Deep velocity structure and anisotropic properties of the asian upper mantle . . . . .</i>	228
<i>Investigation of the boundary and internal fault zones of Tunka basin (Baikal rift system) using HVSR method . . . . .</i>	231
<i>High Topography and Deformation in Continental Interiors: Structure and Geodynamics of Central Mongolia . . . . .</i>	235
<i>Thickness of earth's crust under broadband stations of Mongolian seismic network . . . . .</i>	236
<i>Estimation of coda wave attenuation in the Hangay Dome, central Mongolia . . . . .</i>	240
<i>Crust and Upper Mantle Structure of Central Mongolia . . . . .</i>	241
<i>Receiver function imaging of crustal and upper mantle structure beneath seismic station Ulan-Ude (Transbaikalia, Russia) . . . . .</i>	247
<i>On conditions of preparation for the catastrophic earthquakes foci within earth crust of central asia . . . . .</i>	250
<i>Deep configuration of the southeast edge of the siberian craton along the passcal_1992 transect . . . . .</i>	256
<i>Vibroseismic sounding of the earth's crust on the profile Baikal – Ulaanbaatar . . . . .</i>	261
<i>Study seismic activity in Khovd region (West part of Mongolia) and seismic velocity 1D model. . . . .</i>	266
 <b><i>Seismic hazard assessment, strong ground motion, attenuation and site effects, microzoning . . . . .</i></b>	<b>271</b>
<i>Seismic hazard assessment of bayan-ulgii aimag: Probabilistic analysis . . . . .</i>	273
<i>Seismic hazard assessment of bayan-ulgii aimag: Microzoning mapping . . . . .</i>	277
<i>Reducing Digitiser Latency for Earthquake Early Warning: New Strategies for Seismic Hardware . . . . .</i>	282
<i>Prediction of seismic effects of large earthquakes in Mongolian-Siberian region by studying the dynamic parameters of earthquakes. . . . .</i>	283
<i>Paleoseismogenic deformations of the central Mongolia and seismic hazard assessment for Ulaanbaatar . . . . .</i>	287
<i>Site effect estimation of Bayan-Ulgii aimag . . . . .</i>	288
<i>Studying of tectonic infringements in seismically active areas of Mongolia. . . . .</i>	290
<i>Effects and Post-Disaster Actions during the 2015 Mw = 8.4 Northern Chile Earthquake. . . . .</i>	295
<i>Weather-climatic changes in the Baikal-Mongol region: analysis and forecast before 2050 . . . . .</i>	296
<i>The seismic microzoning study in Mongolia: the example of Ulgii city, center of Bayan-Ulgii aimag. . . . .</i>	302
<i>Seismic hazard assessment of bayan-ulgii aimag: Deterministic analysis . . . . .</i>	306
<i>Seismic safety assessment of earth dams. . . . .</i>	309
<i>Seismic microzoning on the joint of geotechnical lands-capes. . . . .</i>	310
<i>Seismic Microzonation: principles and practices (for example, the city of Ulan-Ude). . . . .</i>	325
<i>Cosmogenic <math>^{36}\text{Cl}</math> geochronology of offset terraces along the Ovacık Fault (Malatya-Ovacık Fault Zone, Eastern Turkey): Implications for the intraplate deformation of the Anatolian scholle . . . . .</i>	330